MIMO-OFDM Transmission Using Complexity Reduced Near ML Detection

Katsuhiro TEMMA† Tetsuya YAMAMOTO† and Fumiyuki ADACHI‡
Dept. of Communication Engineering, Graduate School of Engineering, Tohoku University
6-6-05 Aza-Aoba, Aramaki, Aoba-ku, Sendai, 980-8579 Japan
†{tenma, yamamoto}@mobile.ecei.tohoku.ac.jp, ‡adachi@ecei.tohoku.ac.jp

***Abstract*—QR decomposition and M-algorithm based near maximum likelihood detection (QRM-MLD) is a promising detection scheme for multiple-input multiple-output (MIMO) - orthogonal frequency division multiplexing (OFDM). However, QRM-MLD requires still high computational complexity. Recently, we proposed a complexity reduced 2-step QRM-MLD for single-carrier (SC) block transmissions. The complexity reduction is achieved by identifying unreliable symbol candidates and pruning them from the tree using the output of minimum mean square error based frequency-domain equalization (MMSE-FDE). The detection order is known to affect the achievable transmission performance. In this paper, we introduce the detection ordering to 2-step QRM-MLD for the application to MIMO-OFDM. We show, by computer simulation, the average packet error rate (PER) performance of 2-step QRM-MLD using the detection ordering to discuss the impact of detection ordering. We also show that 2-step QRM-MLD using the detection ordering can reduce the complexity compared to QRM-MLD while keeping the same PER performance.**

Keywords-component; OFDM, MIMO, MLD, MMSED, QR decomposition, M-algorithm, detection ordering

I. INTRODUCTION

To provide the broadband services with limited bandwidth, highly spectrum-efficient transmission technique is demanded. Since the broadband wireless channel is composed of many propagation paths with different time delays, the channel becomes severely frequency-selective [1]. Recently, signal transmission using multiple-input multiple-output (MIMO) [2] and orthogonal frequency division multiplexing (OFDM) [3] has been attracting much attention.

Although the maximum likelihood detection (MLD) [4] can significantly improve the transmission performance of MIMO-OFDM, MLD requires very high computational complexity. To remedy this problem, QR decomposition and M-algorithm based near MLD (QRM-MLD) [5] was proposed and followed by further complexity reduced QRM-MLD schemes [6, 7].

Recently, we proposed the complexity reduced 2-step QRM-MLD for single-carrier (SC) block transmission [8, 9]. The complexity reduction is achieved by identifying unreliable symbol candidates and pruning them from the tree using the output of minimum mean square error (MMSE) based frequency-domain equalization (FDE) [10, 11].

In QRM-MLD, the signal detection ordering has significant impact on the achievable transmission performance. In this paper, we introduce the detection ordering to 2-step QRM-MLD for the application to MIMO-OFDM. We consider two ordering methods in this paper: the number of remaining symbol candidates based ordering [12] and sorted QR decomposition (SQRD) [13].

The remainder of this paper is organized as follows. In Sect. II, MIMO-OFDM transmission model is presented. Section III describes 2-step QRM-MLD using detection ordering. In Sect. IV, we evaluate by computer simulation the packet error rate (PER) performance and discuss the impact of detection ordering. We also discuss the computational complexity. Section V offers some conclusions.

II. TRANSMISSION MODEL

The MIMO-OFDM transmission model is illustrated in Fig. 1. Throughout the paper, the T_s symbol-spaced discrete time representation is used. At the transmitter, the information bit sequence is coded, punctured, interleaved and the coded bit sequence is serial-to-parallel (S/P) converted to N_t parallel bit sequences, where N_t is the number of transmit antennas. Each bit sequence is data-modulated and divided into a sequence of signal blocks of N_c symbols. The data symbol block of n_tth transmit antenna can be expressed using the vector form as $\mathbf{d}_{n_t} = [d_{n_t}(0),\ldots,d_{n_t}(N_c-1)]^T$ ($[.]^T$ is the transpose operation). Next, N_c-point inverse discrete Fourier transform (IDFT) is applied to $\mathbf{d}_{n_t}$ and OFDM symbol block composed of N_c symbols $\mathbf{s}_{n_t} = [s_{n_t}(0),\ldots,s_{n_t}(N_c-1)]^T$ is made. Then, the last N_g symbols of each block are copied as a cyclic prefix (CP) and inserted into the guard interval (GI) placed at the beginning of each block.

We assume a symbol-spaced frequency-selective fading channel composed of L distinct propagation paths. The channel impulse response between the n_tth transmit antenna and the n_rth receive antenna $h_{n_r,n_t}(\tau)$ is given by

$$h_{n_r,n_t}(\tau) = \sum_{l=0}^{L-1} h_{n_r,n_t}^{(l)} \delta(\tau - \tau_{n_r,n_t}^{(l)}), \quad (1)$$

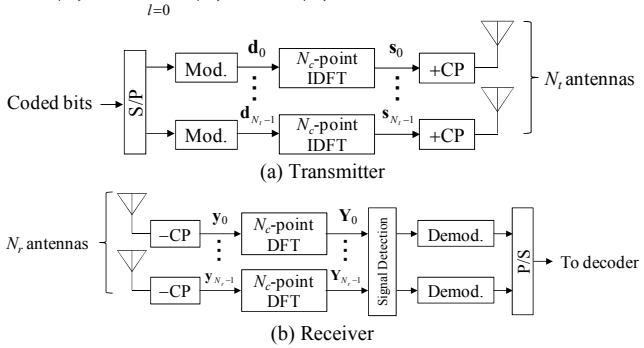

Figure 1. MIMO-OFDM transmission model.

where $h_{n_r,n_t}^{(l)}$ is the complex-valued path gain with $E[\sum_{l=0}^{L-1}|h_{n_r,n_t}^{(l)}|^2]=1$ and $\tau_{n_r,n_t}^{(l)}$ is the time delay of the lth path between the n_tth transmit antenna and the n_rth receive antenna.

At the receiver, N_c-point DFT is applied to the CP-removed received signal block at each received antenna. The received signal vector composed of kth element of frequency-domain received signal at each received antenna $\mathbf{Y}(k)=[Y_0(k),\ldots,Y_{N_r-1}(k)]^T$ can be represented as

$$\mathbf{Y}(k)=\sqrt{\frac{2E_s}{T_s}}\mathbf{H}(k)\mathbf{d}(k)+\mathbf{N}(k). \quad (2)$$

E_s is the data symbol energy. $\mathbf{H}(k)$ is the $N_r\times N_t$ frequency-domain channel gain matrix and its (n_r, n_t) element can be represented as $H_{n_r,n_t}(k)=\sum_{l=0}^{L-1}h_{n_r,n_t}^{(l)}\exp(-j2\pi k\tau_{n_r,n_t}^{(l)}/N_c)$. $\mathbf{d}(k)=[d_0(k),\ldots,d_{N_t-1}(k)]^T$ is the data symbol vector composed of kth element of transmitted data block at each transmit antenna. $\mathbf{N}(k)=[N_0(k),\ldots,N_{N_r-1}(k)]^T$ is the frequency-domain noise vector whose elements are independent zero-mean additive white Gaussian variables having the variance $2N_0/T_s$, N_0 is the one-sided power spectrum density of the additive white Gaussian noise. Based on Eq. (2), signal detection is carried out on each subcarrier.

III. 2-STEP QRM-MLD

A. Symbol candidate selection using MMSED output

First, the *a posteriori* probability of each symbol candidate is calculated by using MMSED output. MMSED is carried out by multiplying $\mathbf{Y}(k)$ by the MMSE weight matrix $\mathbf{W}(k)$ as [1]

$$\tilde{\mathbf{d}}(k)=\mathbf{W}(k)\mathbf{Y}(k), \quad (3)$$

where $\tilde{\mathbf{d}}(k)=[\tilde{d}_0(k),\ldots,\tilde{d}_{N_t-1}(k)]^T$ is the MMSED output vector and $\mathbf{W}(k)$ is given as

$$\mathbf{W}(k)=\left[\mathbf{H}^H(k)\mathbf{H}(k)+\left(\frac{E_s}{N_0}\right)^{-1}\mathbf{I}_{N_t}\right]^{-1}\mathbf{H}^H(k), \quad (4)$$

$\mathbf{I}_{N_t}$ is the $N_t\times N_t$ unit matrix and $[.]^H$ represents the Hermitian transpose operation. MMSED output $\tilde{d}_{n_t}(k)$ for the transmitted data symbol at n_tth transmit antenna on the kth subcarrier can be represented as

$$\tilde{d}_{n_t}(k)=\sqrt{\frac{2E_s}{T_s}}\left(\sum_{i=0}^{N_r-1}W_{n_t,i}(k)H_{i,n_t}(k)\right)d_{n_t}(k)+\mu_{IAI,n_t}(k)+\mu_{noise,n_t}(k). \quad (5)$$

In Eq. (5), $W_{n_t,i}(k)$ is the (n_t, i) element of $\mathbf{W}(k)$, $\mu_{IAI,n_t}(k)$ and $\mu_{noise,n_t}(k)$ are respectively the residual inter-antenna interference (IAI) and noise. For simplicity, $\tilde{d}_{n_t}(k)$ is normalized by $A=\sqrt{2E_s/T_s}\sum_{i=0}^{N_r-1}W_{n_t,i}(k)H_{i,n_t}(k)$ as

$$\tilde{d}'_{n_t}(k)=d_{n_t}(k)+\mu'_{IAI,n_t}(k)+\mu'_{noise,n_t}(k), \quad (6)$$

$$\mu'_{IAI,n_t}(k)=A^{-1}\sqrt{\frac{2E_s}{T_s}}\sum_{i=0\neq n_t}^{N_t-1}\left[\sum_{j=0}^{N_r-1}W_{n_t,j}(k)H_{j,i}(k)\right]d_i(k), \quad (7)$$

$$\mu'_{noise,n_t}(k)=A^{-1}\sum_{i=0}^{N_r-1}W_{n_t,i}(k)N_i(k). \quad (8)$$

In this paper, $\mu'_{IAI,n_t}(k)$ and $\mu'_{noise,n_t}(k)$ are modeled as independent zero-mean complex Gaussian variables [14]. The residual IAI plus noise $\mu_{n_t}(k)=\mu'_{IAI,n_t}(k)+\mu'_{noise,n_t}(k)$ can be treated as a new zero-mean complex Gaussian variable. The variance σ^2_{μ,n_t} of $\mu_{n_t}(k)$ can be calculated as

$$\sigma^2_{\mu,n_t}=\frac{1}{2}E[|\mu_{n_t}(k)|^2]=\frac{1}{2}\{E[|\tilde{d}'_{n_t}(k)|^2]-E[|d_{n_t}(k)|^2]\}. \quad (9)$$

Equation (9) calculates the variance of difference between the MMSED output and desired signal. The first and second terms can be obtained as

$$E[|\tilde{d}'_{n_t}(k)|^2]=A^{-2}\frac{E_s}{T_s}\left\{\sum_{i=0}^{N_r-1}W_{n_t,i}(k)H_{i,n_t}(k)\right\}^*, \quad (10)$$

$$E[|d_{n_t}(k)|^2]=A^{-2}\frac{E_s}{T_s}\left|\sum_{i=0}^{N_r-1}W_{n_t,i}(k)H_{i,n_t}(k)\right|^2, \quad (11)$$

where $[.]^*$ is the complex conjugate operation. Therefore, the variance σ^2_{μ,n_t} of $\mu_{n_t}(k)$ can be obtained as

$$\sigma^2_{\mu,n_t}=\frac{1}{2}\frac{1-\sum_{i=0}^{N_r-1}W_{n_t,i}(k)H_{i,n_t}(k)}{\sum_{i=0}^{N_r-1}W_{n_t,i}(k)H_{i,n_t}(k)}. \quad (12)$$

The *a posteriori* probability of each symbol candidate can be calculated by using σ^2_{μ,n_t}.

From Bayes' theorem, when the MMSED output is obtained, the *a posteriori* probability of a symbol candidate c_i (i=0~X–1, X is the modulation level) can be calculated as

$$P(c_i|\tilde{d}'_{n_t}(k))=\frac{P(c_i)p(\tilde{d}'_{n_t}(k)|c_i)}{p(\tilde{d}'_{n_t}(k))}, \quad (13)$$

where $P(c_i)$ is the probability that a symbol candidate c_i is transmitted, $p(\tilde{d}'_{n_t}(k)|c_i)$ is the conditional probability density function (pdf) given as

$$p(\tilde{d}'_{n_t}(k)|c_i)=\frac{1}{2\pi\sigma^2_{\mu,n_t}}\exp\left(-\frac{|\tilde{d}'_{n_t}(k)-c_i|^2}{2\sigma^2_{\mu,n_t}}\right), \quad (14)$$

and $p(\tilde{d}'_{n_t}(k))$ is the pdf of $\tilde{d}'_{n_t}(k)$. In this paper, we assume that all the symbol candidates are transmitted with same probability, and therefore, $P(c_i)$=1/X for i=0~X–1. Then, assuming $P(c_i)$=1/X, $P(c_i|\tilde{d}'_{n_t}(k))$ can be calculated as

$$P(c_i|\tilde{d}'_{n_t}(k))=\frac{P(c_i)p(\tilde{d}'_{n_t}(k)|c_i)}{\sum_{j=0}^{X-1}p(\tilde{d}'_{n_t}(k)|c_j)P(c_j)}=\frac{p(\tilde{d}'_{n_t}(k)|c_i)}{\sum_{j=0}^{X-1}p(\tilde{d}'_{n_t}(k)|c_j)}. \quad (15)$$

Next, symbol candidate selection is carried out. Figure 2 shows the process of symbol candidate selection. The symbol candidates are selected in descending order of the *a posteriori*

probability and the accumulated *a posteriori* probability is calculated. This process continues while the accumulated *a posteriori* probability exceeds the threshold α set in advance.

If α is set too large, few symbol candidates are discarded and therefore, the computational complexity of 2-step QRM-MLD cannot be reduced from QRM-MLD a lot. However, the use of too small α leads to the transmission performance degradation. In this paper, we set α to satisfy that the average PER performance degradation due to the symbol candidate selection is within the 10% from the average PER of MLD at each average received E_s/N_0 by prior computer simulation.

After symbol candidate selection, the computational complexity of QR decomposition can be reduced [9]. As shown in Fig. 3, the number $N_{cand}^{n_t}(k)$ of symbol candidates corresponding to $d_{n_t}(k)$ may be limited to only one. These symbols can be detected by using MMSED output without tree search and therefore, $d_{n_t}(k)$ with $N_{cand}^{n_t}(k)=1$ can be canceled from received signal by assuming the hard decision result of MMSED as correct. In this process, the column element of channel matrix $\mathbf{H}(k)$ corresponding to $d_{n_t}(k)$ with $N_{cand}^{n_t}(k)=1$ can be treated as zero, so the size of channel matrix can be reduced from $N_r \times N_t$ to $N_r \times (N_t - C)$, where C is the number of $d_{n_t}(k)$ with $N_{cand}^{n_t}(k)=1$. Hence, the number of complex multiplications required for the QR decomposition can be reduced from $N_r N_t^2$ to $N_r(N_t-C)^2$.

B. Detection ordering

In QRM-MLD, the detection order of transmitted symbol has much effect on the accuracy of signal detection in M-algorithm, especially when the number M of surviving paths in M-algorithm at each stage is small. In this paper, we compare the number $N_{cand}^{n_t}(k)$ of remaining symbol candidate based ordering ($N_{cand}^{n_t}(k)$ based ordering) [12] and SQRD [13] in 2-step QRM-MLD.

In $N_{cand}^{n_t}(k)$ based ordering, the detection order is determined by sorting the symbols $d_0(0) \sim d_{N_t-1-C}(k)$ in ascending order of $N_{cand}^{n_t}(k)$. In this process, the number of paths in early stages can be reduced, so the path pruning in early stage of M-algorithm becomes less frequent. Therefore, the performance degradation caused by pruning the path with low-accurate can be reduced.

SQRD prevent the lower right of diagonal element of upper triangular matrix which has much effect on the accuracy of path metric in early stage from dropping. By using SQRD, the accuracy of path metric in early stage of M-algorithm can be improved and therefore, the detection accuracy in M-algorithm becomes better.

C. QRM-MLD

After symbol candidate selection and applying the detection ordering, QRM-MLD is carried out. First, QR decomposition is applied to $N_r \times (N_t - C)$ channel matrix $\hat{\mathbf{H}}(k)$ after applying the method to reduce the computation of QR decomposition and detection ordering as

$$\hat{\mathbf{H}}(k) = \hat{\mathbf{Q}}(k)\hat{\mathbf{R}}(k), \tag{16}$$

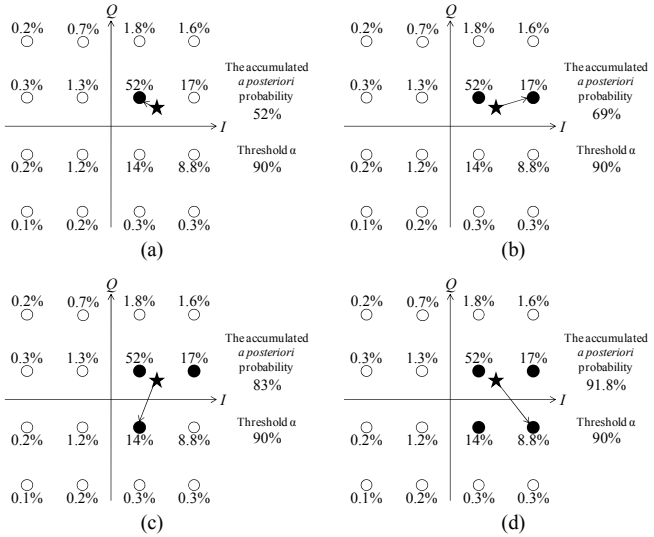

Figure 2. Symbol candidate selection in 2-step QRM-MLD.

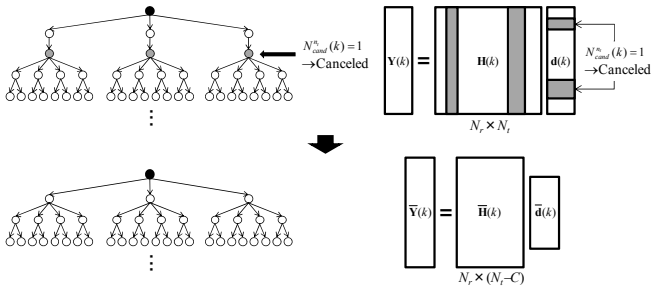

Figure 3. Complexity reduction method of QR decomposition.

where $\hat{\mathbf{Q}}(k)$ is the $N_r \times (N_t - C)$ matrix satisfying $\hat{\mathbf{Q}}^H(k)\hat{\mathbf{Q}}(k) = \mathbf{I}_{N_t - C}$ and $\hat{\mathbf{R}}(k)$ is the $(N_t - C) \times (N_t - C)$ upper triangular matrix. Then, multiplying $\bar{\mathbf{Y}}(k)$ which is the received signal vector after cancelling $d_{n_t}(k)$ with $N_{cand}^{n_t}(k)=1$ by $\hat{\mathbf{Q}}^H(k)$, the transformed received signal $\mathbf{Z}(k) = [Z_0(k), \ldots, Z_{N_t-1-C}(k)]^T$ is obtained as

$$\begin{aligned}\mathbf{Z}(k) &= [Z_0(k), \ldots, Z_{N_t-1-C}(k)]^T = \sqrt{\frac{2E_s}{T_s}}\hat{\mathbf{Q}}^H(k)\bar{\mathbf{Y}}(k) \\ &= \sqrt{\frac{2E_s}{T_s}}\begin{bmatrix} \hat{R}_{0,0}(k) & \cdots & \hat{R}_{0,N_t-1-C}(k) \\ & \ddots & \vdots \\ & & \hat{R}_{N_t-1-C,N_t-1-C}(k) \end{bmatrix}\begin{bmatrix} \hat{d}_0(k) \\ \vdots \\ \hat{d}_{N_t-1-C}(k) \end{bmatrix}, \\ &\quad + \hat{\mathbf{Q}}^H(k)\mathbf{N}(k)\end{aligned} \tag{17}$$

where $\hat{\mathbf{d}} = [\hat{d}_0(k), \ldots, \hat{d}_{N_t-1-C}(k)]^T$ is the $(N_t - C) \times 1$ data symbol sequence vector after omitting the $d_{n_t}(k)$ with $N_{cand}^{n_t}(k)=1$ from $\mathbf{d}(k)$ and applying the detection ordering.

M-algorithm is composed of $N_t - C$ stages. In each stage, the best M paths are selected as surviving paths by comparing the path metrics based on the squared Euclidean distance for all surviving paths and are passed to the next stage. In the case of uncoded transmission, the data demodulation is carried out by tracing back the path having the smallest path metric at the last stage. On the other hand, in the case of coded transmission, the log likelihood ratio (LLR) is used as the soft-input in the

decoder. When QRM-MLD is used, however, the LLR values cannot be directly computed since surviving paths at the last stage do not necessarily contain both 1 and 0 for every coded bit. In this paper, we apply the LLR calculation method proposed in [15]. The approximate LLR values are computed at every stage by using path metric and updated successively as tree search progresses. If the LLR value cannot be computed at the last stage, the recently updated approximate LLR value at the upper stage is used. In addition, when 2-step QRM-MLD is used, LLR cannot be computed even if the LLR estimation method noted above in some cases because of the symbol candidate selection. In this case, LLR is computed from MMSED output.

IV. Computer Simulation

We evaluate the average PER performance of 4×4 MIMO-OFDM spatial multiplexing using 2-step QRM-MLD and computational complexity by computer simulation. We assume 16QAM data modulation. We employ a rate 1/3 turbo encoder using two (13, 15) recursive systematic convolutional (RSC) component encoders. The two parity sequences from the turbo encoder are punctured to obtain rate-3/4 turbo codes. Log-MAP decoding with 6 iterations is assumed. The length of packet is 1024 bits. The number of subcarriers is N_c=64 and GI size is N_g=16 per each antenna. The channel is assumed to be a frequency-selective block Rayleigh fading channel having symbol-spaced L=16-path uniform power delay profile. Ideal channel estimation is assumed.

The comparison of detection ordering methods is shown in Fig. 4. In this paper, we set the number of M to satisfy that the degradation of average E_s/N_0 from MLD is within the 1dB at the average PER=10^{-3}. From Fig. 4, we can see that the average PER performance is improved by applying detection ordering. When the value of M is small (M=8), $N_{cand}^{n_t}(k)$ based ordering is efficient compared to SQRD. This is because the path pruning in early stage of M-algorithm becomes less frequent even if small value of M is used by applying $N_{cand}^{n_t}(k)$ based ordering. However, in order to satisfy that the degradation of average E_s/N_0 from MLD is within the 1dB at the average PER=10^{-3}, M=20 and M=16 are respectively needed when $N_{cand}^{n_t}(k)$ based ordering and SQRD are used. In both cases, the value of M has to be set to more than 16. This means that the path pruning is not occurred at least in first stage of M-algorithm because 16QAM is used. Therefore, $N_{cand}^{n_t}(k)$ based ordering is less effective when the value of M is not small. In addition, when the symbol candidate is not much limited, the effect of $N_{cand}^{n_t}(k)$ based ordering becomes less. On the other hand, SQRD prevent the lower right of diagonal element of upper triangular matrix from dropping and hence, SQRD is effective even if the symbol candidate is not much limited. For these reasons, SQRD is more effective compared to $N_{cand}^{n_t}(k)$ based ordering when M is not set to small value. In this paper, we use SQRD because it can reduce the required value of M.

Figure 5 shows the average PER performance comparison between 2-step QRM-MLD and conventional QRM-MLD. For comparison, the PER performance of MMSED and MLD are also shown. QRM-MLD requires M=20 to satisfy that the degradation of average E_s/N_0 from MLD is within the 1dB at the average PER=10^{-3}. On the other hand, M=16 is enough when 2-step QRM-MLD is used. This is because the path pruning in early stage of M-algorithm becomes less frequent owing to the symbol candidate selection.

TABLE I. Computer Simulation Condition

Transmitter	Modulation	16QAM
	No. of transmit antennas	N_t=4
	No. of subcarriers	N_c=64
	GI size	N_g=16
Coding	Packet size	1024 bits
	Encoder	R_t=1/3 (13,15) RSC encoder
	Coding rate	R=3/4
	Decoder	Log MAP (6 iterations)
Channel	Fading type	Frequency-selective block Rayleigh
	Power delay profile	L=16-path uniform power delay profile
	Time delay	$\tau_l=l$ (l=0~L−1)
Receiver	No. of receive antennas	N_r=4
	Channel estimation	Ideal

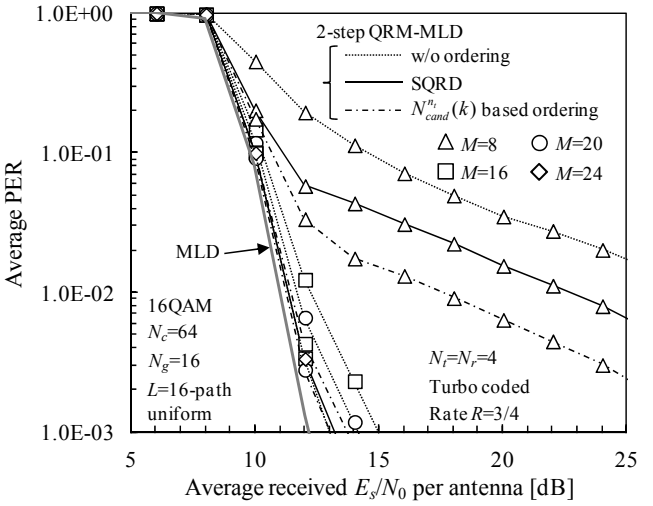

Figure 4. The effect of detection ordering methods comparison.

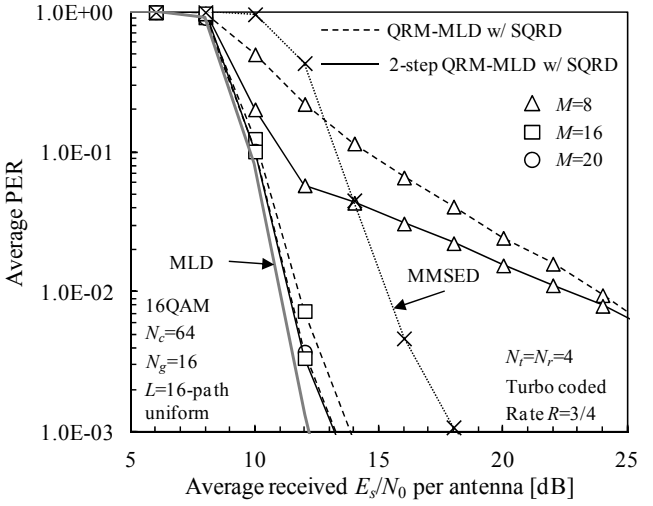

Figure 5. PER performance comparison.

In Table II, the average number of complex multiplications is shown. The 2-step QRM-MLD requires additional computation of MMSED and cancellation of symbols with $N_{cand}^{n_t}(k)=1$ from received signal. However, the complexity of QR decomposition and required value of M can be reduced and therefore, a total computational complexity of 2-step QRM-MLD is reduced compared to QRM-MLD. Figure 6 shows the average number of $N_{cand}^{n_t}(k)$ and C and Fig. 7 shows the average number of complex multiplications required for detecting one subcarrier. In the region that average received E_s/N_0 is less than 8dB, α is set to 0 and so only MMSED is performed because the PER performance difference between MLD and MMSED is almost negligible. From Figs. 6 and 7, we can see that 2-step QRM-MLD can reduce the computational complexity compared to QRM-MLD. For example, the computational complexity of 2-step QRM-MLD is 40% of that of QRM-MLD for achieving average PER $\approx 10^{-3}$ (average received E_s/N_0 per antenna is 12dB).

V. CONCLUSIONS

In this paper, we introduced the detection ordering to 2-step QRM-MLD for the application to MIMO-OFDM. We considered two detection ordering methods: the number of remaining symbol candidates based ordering and SQRD. We evaluated, by computer simulation, the average PER performance and complexity. We showed that SQRD is more efficient compared to the former when M is relatively large. We also showed that 2-step QRM-MLD using SQRD can reduce the number of symbol candidates to be searched per stage and required number M of surviving paths and therefore, lower the complexity than the conventional QRM-MLD.

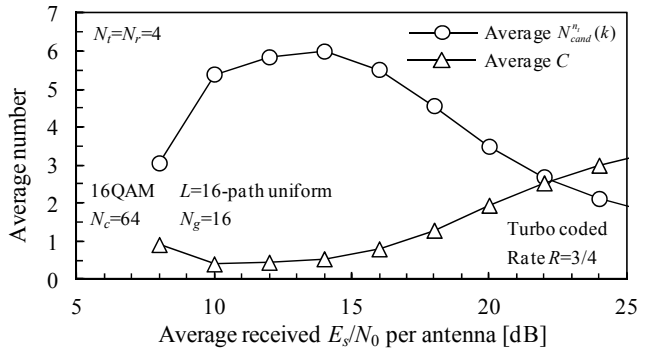

Figure 6. Average number of $N_{cand}^{n_t}(k)$ and C.

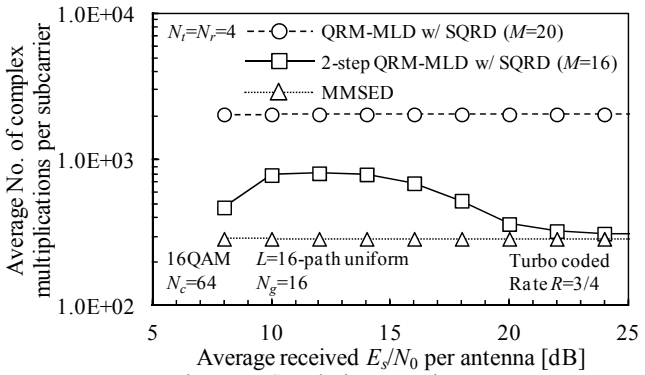

Figure 7. Complexity comparison.

TABLE II. THE AVERAGE NUMBER OF COMPLEX MULTIPLICATIONS

	QRM-MLD	2-step QRM-MLD
$\mathbf{W}(k)$ computation		$2N_t^2N_r+N_t^3$
$\mathbf{W}(k)$ multiplication		N_tN_r
Computation of σ^2_{μ,n_t}		N_tN_r
Symbol candidate selection		N_tX
Cancellation of signals with $N_{cand}^{n_t}(k)=1$		CN_r
SQRD	$(3N_t^2N_r-N_tN_r)/2$	$\{3(N_t-C)^2N_r-(N_t-C)N_r\}/2$
Computation of $\mathbf{Q}^H(k)\mathbf{Y}(k)$	N_tN_r	$(N_t-C)N_r$
Path metric computation	$2X+\sum_{i=2}^{N_t}\left[(i-1)\min(X^{i-1},M)+2\min(X^i,MX)\right]$	$2V+\sum_{i=2}^{N_t-C}\left[(i-1)\min(V^{i-1},M)+2\min(V^i,MX)\right]$ $V=E[N_{cand}^{n_t}(k)]$

REFERENCES

[1] J. G. Proakis and M. Salehi, *Digital communications*, 5th ed., McGraw-Hill, 2008.

[2] G. J. Foschini and M. J. Gans, "On limit of wirelesscommunications in a fading environment when using multiple antennas," Wireless Personal Commun., Vol.6, No. 3, pp. 311-335, 1998.

[3] R. Van Nee and R. Prasad, *OFDM for Wireless Multimedia Communications*, Artech House, 2000.

[4] A. van Zelst, R. van Nee, and G. A. Awater, "Space division multiplexing (SDM) for OFDM systems," Proc. IEEE 51st Vehicular Technology Conference (VTC2000-Spring), Vol. 2, pp. 1070-1074, May 2000.

[5] L. J. Kim and J. Yue, "Joint channel estimation and data detection algorithms for MIMO-OFDM systems," Proc. Thirty-Sixth Asilomar Conference on Signals, System and Computers, pp. 1857-1861, Nov. 2002.

[6] H. Kawai, K. Higuchi, N. Maeda, and M. Sawahashi, "Adaptive control of surviving symbol replica candidates in QRM-MLD for OFDM MIMO multiplexing" IEEE J. Select. Areas Commun., Vol. 24, No. 6, pp. 1130-1140, Jun. 2006.

[7] S. Nagayama and T. Hattori, "A proposal of QRM-MLD for reduced complexity of MLD to detect MIMO signals in fading environment," Proc. IEEE 64th Vehicular Technology Conference (VTC2006-Fall), Sept. 2006.

[8] K. Temma, T. Yamamoto, and F. Adachi, "Computationally efficient 2-step QRM-MLD for single-carrier transmissions," Proc. The IEEE International Conference on Communication Systems (IEEE ICCS 2010), Nov. 2010.

[9] K. Temma, T. Yamamoto, and F. Adachi, "Improved decision 2-step QRM-ML block signal detection for single-carrier Transmission," Proc. IEEE 74th Vehicular Technology Conference (VTC2011-Fall), Sep. 2011.

[10] D. Falconer, S. L. Ariyavisitakul, A. Benyamin- Seeyar, and B. Edison, "Frequency domain equalization for single-carrier broadband wireless systems," IEEE Commun. Mag., Vol. 40, No. 4, pp. 58-66. Apr. 2002.

[11] F. Adachi, T. Sao, and T. Itagaki, "Performance of multicode DS-CDMA using frequency domain equalization in a frequency selective fading channel," IEE Electronics Letters, Vol. 39, No.2, pp. 239-241, Jan. 2003.

[12] K. Temma, T. Yamamoto, and F. Adachi, "2-step QRM-MLBD using Detection Ordering for Single-Carrier Transmission," Proc. IEEE 75th Vehicular Technology Conference (VTC2012-Spring), May 2012.

[13] D. Wübben, R. Böhnke, J. Rinas, V. Kühn, and K. D. Kammeyer, "Efficient algorithm for decoding layered space-time codes," IEE Electronics Letters, Vol. 37, No. 22, pp. 1348-1350, Oct. 2001.

[14] H. V. Poor and S. Verdu, "Probability of error in MMSE multiuser detection," *IEEE Trans. Inf. Theory*, Vol. 43, pp. 858-871, May 1997.

[15] W. Shin, H. Kim, M Son, and H. Park, "An improved LLR computation for QRM-MLD in coded MIMO systems," Proc. IEEE 66th Vehicular Technology Conference (VTC2007-Fall), pp.447-451, Oct. 2007.